Comparison of three approaches to determine the projected area in contact from finite element Berkovich nanoindentation simulations in tungsten

IOP Conf. Series: Materials Science and Engineering **257** (2017) 012013 doi:10.1088/1757-899X/257/1/012013

Comparison of three approaches to determine the projected area in contact from finite element Berkovich nanoindentation simulations in tungsten

T Volz[1,3], R Schwaiger[3], J Wang[3] and S M Weygand[2]

[1] Institute of Applied Research, Karlsruhe University of Applied Sciences, Moltkestraße 30,
76133 Karlsruhe, Germany
[2] Faculty of Mechanical Engineering and Mechatronics, Karlsruhe University of Applied Sciences, Moltkestraße 30, 76133 Karlsruhe, Germany
[3] Institute for Applied Materials (IAM), Karlsruhe Institute of Technology (KIT), Hermann-von-Helmholtz-Platz 1, 76344 Eggenstein-Leopoldshafen, Germany

*Corresponding author: tillmann.volz@hs-karlsruhe.de

Abstract. Nanoindentation nowadays is a standard method for the mechanical characterization of thin films and small volumes of material. One of the most meaningful parameters determined in nanoindentation experiments and simulations is the hardness of the tested material. For its determination, the knowledge of the exact value of the projected area in contact between the indenter and the specimen is essential. Inaccurate results for the projected area will result in noticeable errors in hardness. The determination of this area in finite element (FE) nanoindentation simulations is challenging because it cannot be determined directly and phenomena like pile-up and geometric imperfections of the indenter have to be considered. Hence, a new method, namely the triangulation method has been developed. It provides a reliable way to determine the projected area in FE-simulations, even under the occurrence of material pile-up. It is based on the nodes in contact between the indenter and the specimen as well as on the coordinates of the nodes. With this information, a Delaunay triangulation and Alpha shapes can be used to calculate the projected area. The triangulation method is compared to two established methods, one following the Oliver-Pharr analysis and the other one based on the computed true area in contact between specimen and indenter. The three methods are applied to results from an elastic-plastic FE simulation. Bland-Altman plots are used to compare the results of the three methods and to validate the triangulation method.

1. Introduction

Tungsten is becoming more and more important as a structural material e.g. in nuclear fusion reactors [1]. However, its brittleness and its brittle-to-ductile transition far above room temperature represent major difficulties to an application, even more so as these properties are strongly influenced by the microstructure of the material [2]. One of the most popular parameters to characterize a material is the hardness determined by nanoindentation. Nowadays nanoindentation is a standard method to investigate the mechanical properties of thin films and small volumes of materials [3-5]. The basic idea of nanoindentation is to measure an elastic-plastic load-displacement curve of a hard spherical, conical or pyramidal diamond indenter with a known geometry penetrating into a softer specimen.

Although this idea is simple in theory, the accurate recording of material-relevant data at sub-micron range, e.g. the load-displacement curve, requires very thorough preparation of the specimen and little influence from the experimental environment. Due to great progress in instrumentation development over the last few decades, nanoindentation is a reliable method to determine a variety of mechanical parameters. These include elastic modulus, hardness, strain hardening exponent, viscoelastic properties and fracture toughness [4], all of them determined from the load-displacement curves that are the "fingerprints" of the tested materials. One meaningful parameter for material scientists and engineers determined in nanoindentation experiments is the hardness H defined by the following equation:

$$H = \frac{P}{A_\mathrm{p}}, \tag{1}$$

where P is the load on the indenter and A_p the projected area in contact. The applied load can be recorded accurately by the nanoindenter, whereas, A_p is the critical parameter for an exact calculation of the hardness. It has to be noted that the given definition of hardness differs from the macroscopic hardness which is defined as the applied force divided by the area of the residual impression, measured optically directly after unloading [4]. Furthermore, the projected area cannot be measured directly like the load P and indentation depth h but has to be calculated indirectly. The direct measurement of the imprints is technically difficult at the length scale relevant to nanoindentation experiments. In case of a perfectly sharp Berkovich indenter, the projected area A_p and the plastic indentation depth h_c are related to each other purely geometrically via the equation:

$$A_\mathrm{P} = 24.5\, {h_\mathrm{c}}^2. \tag{2}$$

Following the Oliver-Pharr analysis [5] the plastic indentation depth h_c can be obtained by the equation:

$$h_\mathrm{c} = h - \varepsilon \frac{P}{S}. \tag{3}$$

Here, S refers to the contact stiffness and ε is a geometry parameter that is 0.75 in case of a Berkovich indenter. To determine the contact stiffness in nanoindentation experiments, continuous stiffness measurement [6] is frequently used. For this dynamic measurement method, a load oscillation with a small amplitude is superimposed on the static load to determine the contact stiffness continuously over the loading portion of the indentation experiment. Alternatively, the contact stiffness can be calculated by determining the slope of an unloading curve after the loading sequence following the Oliver-Pharr analysis [5]:

$$S = \frac{\mathrm{d}P}{\mathrm{d}h}. \tag{4}$$

Beside nanoindentation experiments, numerical simulations of nanoindentation are used to investigate the mechanical properties and deformation behavior of small scale specimens. Simulations of nanoindentation processes can support experiments and help to understand the deformation behavior and stress distributions. FE simulations along with advanced plasticity models like crystal plasticity or strain gradient plasticity have turned out to be a convenient approach for a detailed description of nanoindentation processes. A variety of methods for the determination of A_p in experiments were developed [5, 7- 10]. In nanoindentation FE simulations, additional information regarding the contact are available and therefore simulations offer the possibility to determine the projected area in contact directly for various geometries of indenters.

In this paper, we compare three approaches to determine the projected area in contact in FE nanoindentation simulations. The first presented method follows the Oliver-Pharr analysis and is based on the simulation of multiple unloading and reloading sequences that allow the determination of the contact stiffness at various indentation depths and thus, the calculation of h_c and A_p. The second method uses the true area in contact which is calculated in the FE software directly together with the geometry of the Berkovich indenter to convert the true area into the projected area in contact. The third method, called triangulation method, has been newly developed in our research and is based on

the contact status of the surface nodes. This method is universally, independent of the occurrence of pile-up (see figure 5) and the shape of the indenter.

2. Finite Element (FE) Modeling

A FE model for indentation was set up to compare the thee proposed methods for the determination of A_p. The FE simulation of the Berkovich indentation was performed with the commercial finite element software Abaqus. The presented three-dimensional model consists of two parts, namely the three-sided Berkovich indenter and the cylindrical specimen with a diameter of 80 µm and a height of 35 µm. The chosen dimensions of the specimen are much larger than the indentation depth to make sure that the stress field does not reach the specimens boundaries. The geometry of the indenter shown in figure 1 is defined by the two half angles of 77.05° and 65.3° which are the values for a Berkovich indenter. As the indenter's deformation is negligible compared to the deformation of the specimen, it is modelled as a non-deformable rigid surface. Like in experiments, the modelled indenter is not perfectly sharp but exhibits a tip radius of 150 nm. The indenter geometry is discretized with 720 rigid four-node elements (R3D4) and 25 rigid three-node elements (R3D3). The specimen shown in figure 1 consists of 33.240 cubic eight-node elements (C3D8R) with reduced integration. The mesh is refined underneath the indenter tip and in the regions where plasticity is expected. Different element sizes were implemented and tested to ensure the convergence of the load-displacement curve. The dimensions of the smallest elements under the tip in the used mesh are about 0.075 µm × 0.075 µm × 0.32 µm. To keep computational time reasonable, the mesh is coarser in regions further away from the contact region. The bottom of the specimen is fixed in all directions while the lateral surface is not restricted. The rotation and lateral movement of the indenter is fixed. Liu et al. [11] have shown, that load and displacement are independent of the friction coefficient. Therefore, the contact between indenter and specimen is treated frictionless.

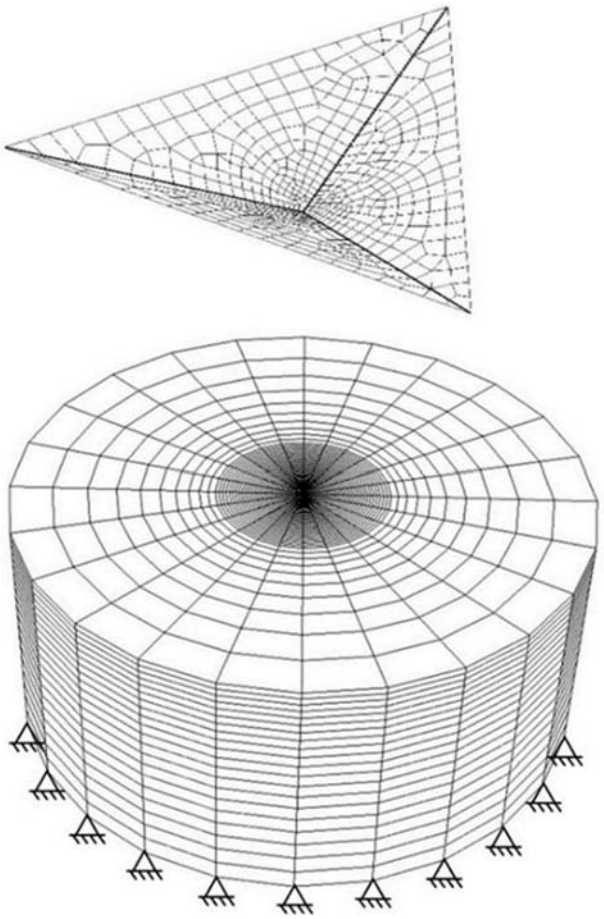

Figure 1. Illustration of the fe-model for the indentation simulation. The rigid Berkovich indenter exhibits the tip radius r = 150 nm.

The mesh of the deformable specimen is refined in the indented region and the bottom is fixed in all directions. The material behavior of tungsten is modelled as elastic-plastic with an elastic modulus E = 408 GPa, Poisson's ratio ν = 0.28 and an initial yield strength of 320 MPa using J_2-plasticity with isotropic hardening. The implemented hardening behavior is given in figure 2. This stress-strain curve is based on the experimental work on tungsten single crystals of Argon and Maloof [12]. The described model is applied to simulate displacement-controlled indentation. Based on the results of the simulation, the three proposed methods for the determination of the projected area can be performed.

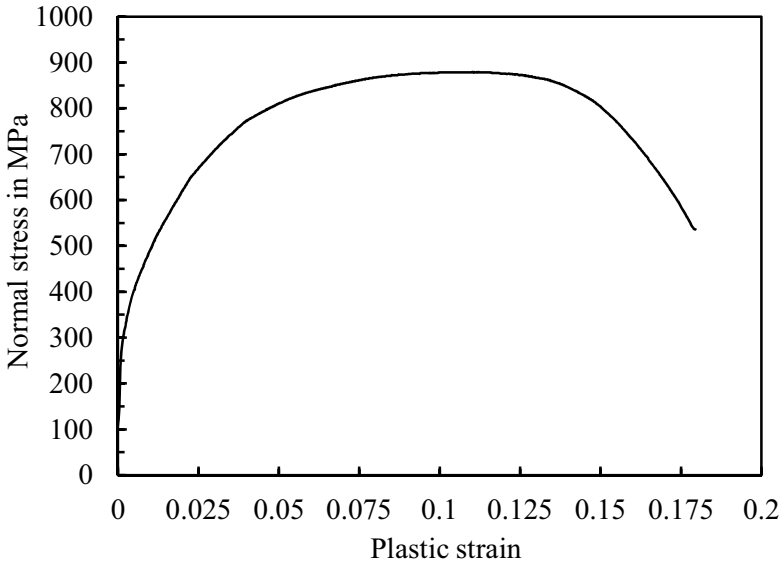

Figure 2. Stress-strain curve implemented in the plastic material model for tungsten.

3. Proposed methods to determine the projected area A_p

In the following section, three methods are presented to determine the projected area of the intender in contact with the specimen in the performed nanoindentation simulations. The aim is to compare these methods among themselves. Thereby the newly developed triangulation method should be validated by comparing its results regarding the projected area in contact A_p and the plastic indentation depth h_c with the established methods based on the Oliver-Pharr analysis and the true area in contact A_C that is determined in Abaqus directly.

3.1. Determination of A_p following the Oliver-Pharr analysis

This method follows the Oliver-Pharr analysis (see equation (3) and (4)) and relies on the assumption that A_p can be calculated from the plastic indentation depth h_c via the purely geometrical relation given in equation (2) for a Berkovich indenter. However, deviations are most likely as the modelled indenter exhibits a tip radius of 150 nm which is not taken into account in equation (2).

In order to obtain the contact stiffness S at different depths according to equation (4), additional unloading sequences were simulated evenly distributed over total depth. Figure 3 shows the computed load-displacement curve with ten unloading and reloading sequences. Based on this load-displacement curve, the slopes of the unloading curves dP/dh are determined via a linear fit to the first four data points of every unloading sequence. Furthermore, the simulations give the corresponding load on the indenter at maximum indentation depth before the unloading sequence. These values together with the geometry parameter ε of 0.75 for a Berkovich indenter are applied in equation (3) to calculate h_c and via equation (2) the corresponding A_p can be calculated. The resulting values are given in table 1.

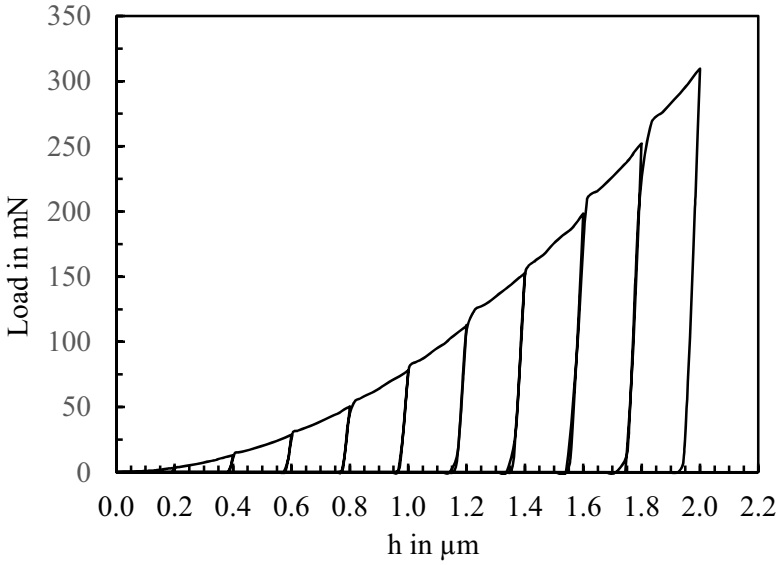

Figure 3. Computed load-displacement curve with ten unloading and reloading sequences during indentation to determine the contact stiffness *S* from the unloading slope.

3.2. Determination of A_p through the true area in contact A_c (A_p-A_c method)

The second method is based on the true area in contact A_c. In contrast to the experimens this value is accessible in the FE simulations and can be determined directly in every increment, i.e. for every indentation depth h. The geometric relation between A_c and A_p is used in this method. In the case of a perfectly sharp Berkovich indenter, A_c equals the lateral surface of the three sided pyramide shown in figure 4 and is related to h_c by:

$$A_c = 27.5\, {h_c}^2. \tag{5}$$

The projected area in contact A_p equals the base surface of the pyramid shown in figure 4 and is calculated following equation (2). Eliminating h_c in equation (2) and (5) leads to the following geometric relation between A_p and A_c:

$$A_p = 0.89\, A_c. \tag{6}$$

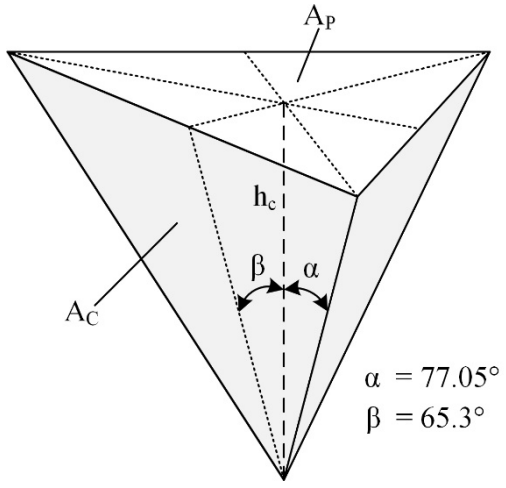

Figure 4. Geometry of the Berkovich indenter.

Applying this procedure to the nanoindentation simulation gives the values for h_c and A_p that are listed in table 1.

3.3. Triangulation method

As mentioned above, the presented two methods require a relation between A_p and h_c or A_c. The given geometric relations (equation (2) and (5)) are only accurate for a Berkovich indenter with a perfectly sharp tip. Furthermore, in soft materials that show high strain-hardening rates, the indentation causes far-field plasticity so that the specimen exhibits plastic deformation further away from the contact impression. This phenomenon is called sink-in and leads to a smaller projected area in contact compared to the original triangle area (see figure 5). Whereas materials with low strain-hardening rates and a large ratio for E_{eff}/σ_y exhibit locally deformation that results in piled up material at the three faces of the indentation (see figure 5). This leads to an underestimation of the real plastic indentation depth h_c and causes a projected area in contact A_c that is larger than the original triangle area and as a result, the hardness calculated from equation (1) is overestimated [7, 13]. Pile-up is not taken into account in the Oliver-Pharr analysis because the plastic indentation depth cannot be larger than the maximum indentation depth following equation (3). However, in the simulation of nanoindentation in tungsten, there is almost no pile-up occurring but one has to be aware of this downside applying the Oliver-Pharr analysis to materials with low strain-hardening rates.

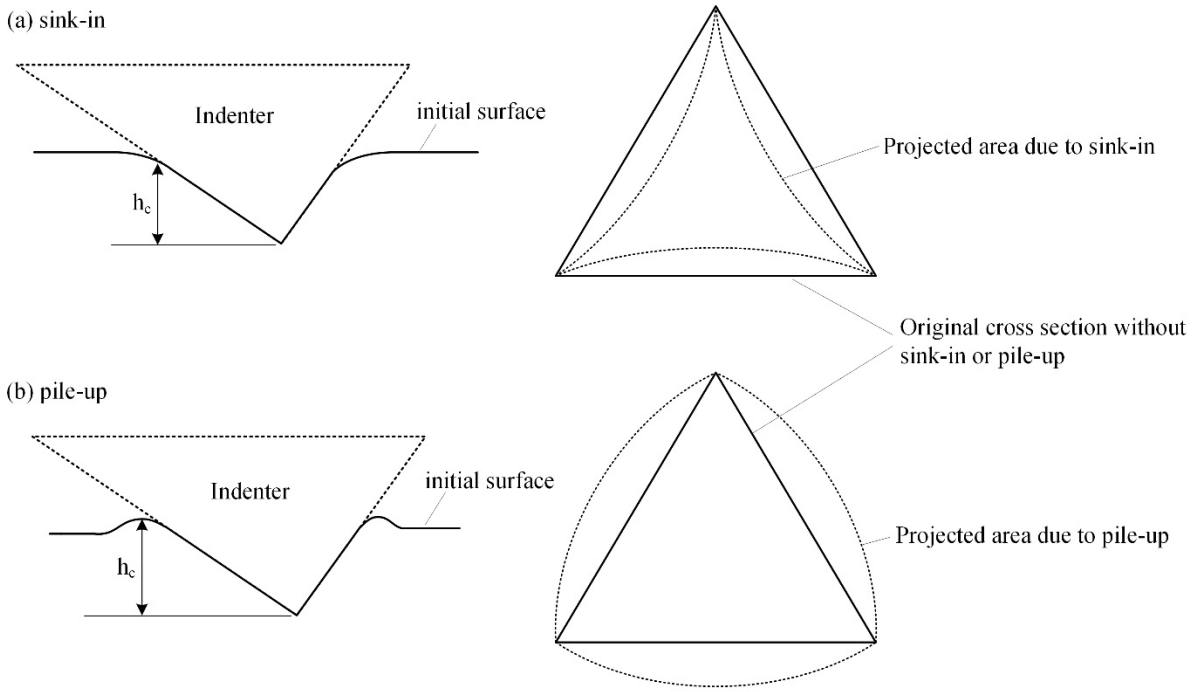

Figure 5. Illustration of sink-in (a) and pile-up (b).

In contrast to experiments, the projected area is directly accessible in the nanoindentation simulations as the positions of all nodes at the surface are known and updated for each indentation depth. A so-called triangulation method is presented which makes use of this information. This method offers a procedure for the determination of the projected area in contact A_p which does not require any geometric relation. It is not restricted to Berkovich indenters, and sink-in and pile-up effects are automatically taken into account. The idea of the newly developed method is based on the contact information of single nodes that are determined in the simulation in every increment. In post-processing, the nodes in contact can be determined and the internal node labels in Abaqus are stored in every increment, i.e. at every indentation depth. With the known node label of all nodes in contact, the node coordinates can be obtained and stored as well. For the determination of the projected area, the node coordinate in the direction of indentation is irrelevant since the projected area is desired. However, the curve that defines the projected area is not a planar curve but a three-dimensional closed

curve that is defined by the connection of all the outer nodes in contact in the simulation. Furthermore, there is not just one plastic indentation depth h_c but a variation along the edge of the projected area [14]. This effect occurs because of the shape of the indenter, sink-in and pile-up and is observed in both, namely simulations as well as in experiments. The projected area of contact between the indenter and the specimen is simply the projection of this three-dimensional curve on a plane normal to the direction of indentation. Figure 6 shows exemplarily the plot of all nodes in contact at an indentation depth of 1400 nm and the projected three-dimensional curve based on the connection of the outer nodes. For the calculation of the desired projected area, a convex hull that includes all nodes in contact could be applied. However, if sink-in occurs the shape of the projected area becomes a concave hull. A more general way is the application of alpha shapes based on the Delaunay triangulation, where the alpha parameter has to be adjusted until the desired shape is found. The result of the triangulation method for the indentation depth of 1400 nm is shown in figure 7. The grey highlighted area as the sum over all triangles represents the desired projected area in contact and can easily be calculated. In summary, the effort for this method is reasonable. It is the most versatile method to determine the projected area in contact since it is independent of the indenter shape and sink-in and pile-up. The method also works for all other standard indenter shapes, independent of blunting and geometric imperfections.

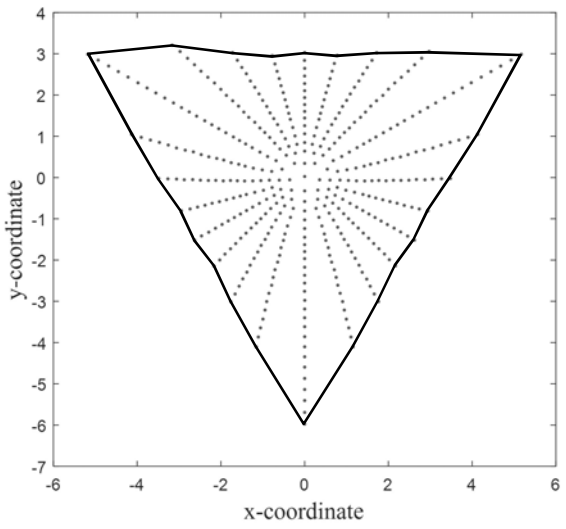

Figure 6. Plot of all nodes in contact at an indentation depth of 1400 nm.

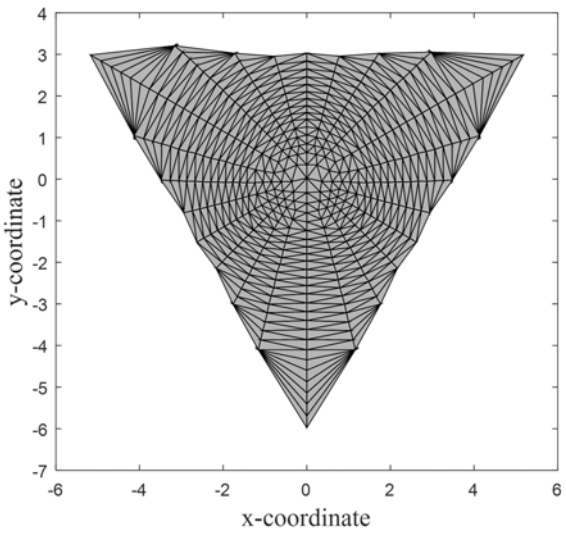

Figure 7. Triangulation to determine A_p based on the nodes in contact.

4. Results and discussion

In the following, the results for the plastic indentation depth h_c and the projected area in contact A_p that are determined in the three presented methods are compared. Table 1 lists the results for h_c and A_p for indentation depths ranging 0.2 µm to 2 µm. The same results are plotted in figure 8 and figure 9 as a function of the indentation depth h. In the Oliver-Pharr analysis, the plotted h_c is calculated with equation (3) and in the A_p-A_c method, h_c is determined with equation (5). In both cases, just one value for the plastic indentation depth is obtained. In the triangulation method, each outer surface node has its own h_c. For a comparison, all these plastic indentation depths determined in the triangulation method are taken to calculate a mean value that is comparable to the two other methods. The values of h_c in the A_p-A_c method are larger than the values of the overall indentation depth h. This is reasonable because a perfectly sharp tip would lead to a smaller true area at the same indentation depth than the true indenter shape with a radius at the tip. Vice versa, the plastic indentation depth in the A_p-A_c method is overestimated since it is determined with the geometric description of the perfect indenter geometry. The occurrence of material pile-up can be another possible explanation for high values of

h_c. However, no material pile-up is observed in the simulation. Moreover, this is confirmed by the results for h_c in the Oliver-Pharr method and the triangulation method. However, it has to be noted that the occurrence of material pile-ups leads to an underestimation of h_c (and of A_p) in the Oliver-Pharr analysis while the triangulation method can handle this properly.

Table 1. Comparison of the results for h_c and A_c determined in the three methods.

Indentation depth in µm	0.2	0.4	0.6	0.8	1.0	1.2	1.4	1.6	1.8	2.0
Oliver-Pharr analysis										
dP/dh in N/mm	560	1186	1766	2358	2965	3722	4172	4973	5616	6262
h_c in µm	0.17	0.39	0.59	0.79	0.98	1.18	1.37	1.57	1.77	1.96
A_p in µm^2	0.95	3.81	8.58	15.26	23.86	34.41	46.78	61.21	77.45	95.66
A_p-A_c method										
h_c in µm	0.22	0.43	0.64	0.84	1.04	1.26	1.42	1.65	1.85	2.02
A_p in µm^2	1.20	4.54	10.23	17.37	27.04	39.75	49.91	67.78	84.60	101.58
Triangulation method										
h_c in µm	0.19	0.39	0.57	0.79	0.98	1.18	1.38	1.60	1.75	1.96
A_p in µm^2	0.99	4.41	9.44	16.18	25.35	34.74	47.52	64.40	80.95	97.36

Figure 9 shows the projected area in contact for all methods. Since no pile-ups occur, only the tip radius could affect the area. We assume that the influence of the radius is negligible and state that all three methods should determine the same values for A_p in the elastic-plastic nanoindentation simulation, the results should be exactly the same in all three methods. This hypothesis is checked with the help of Bland-Altman plots given in the appendix. They prove that the triangulation method is a versatile method for determining the projected area in contact.

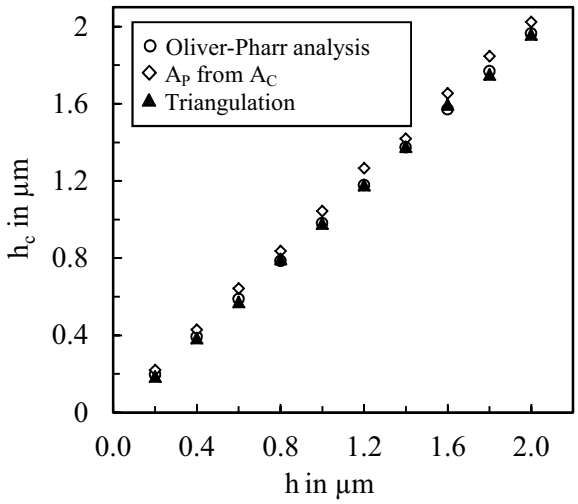

Figure 8. Comparison of the plastic indentation depth determined by the three methods.

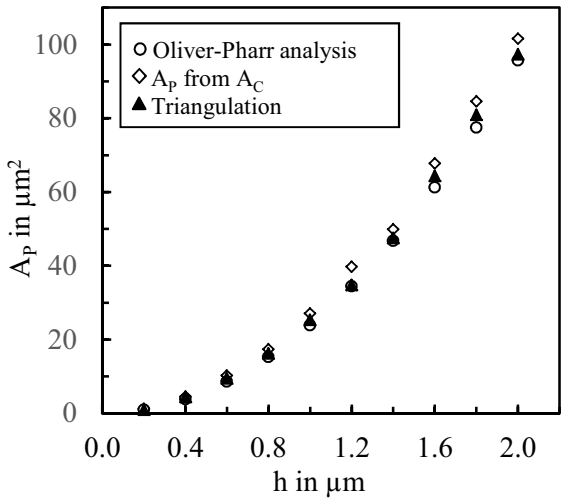

Figure 9. Comparison of the projected area in contact determined by the three methods.

The values of A_p obtained with the triangulation method are used together with the calculated load-displacement curve shown in figure 10 to calculate the nanoindentation hardness according to equation (1). The resulting hardness is given in figure 11. As expected, the hardness is constant over the

indentation depth. Nanoindentation experiments in tungsten single crystals indicate an increase of the hardness with decreasing indentation depth at small scale, the so-called indentation size effect (ISE). Nix and Gao established a relation between hardness and indentation depth [15]. As the implemented elastic-plastic material model is a standard local version, it cannot describe size dependent behavior. An approach for the simulation of the ISE is the implementation of strain gradient plasticity (SGP) into the simulation to describe the strain gradients underneath the tip of the indenter.

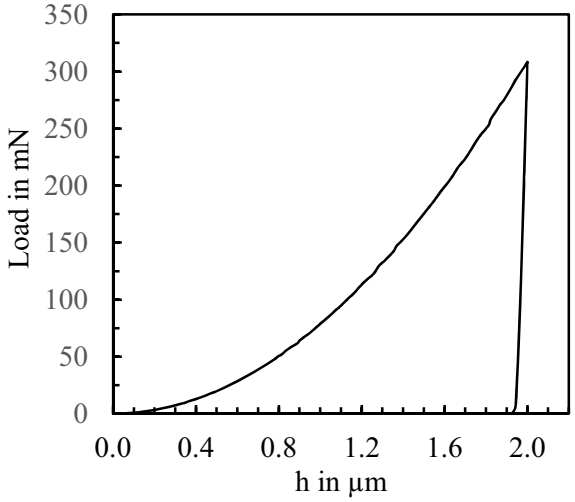

Figure 10. Computed load-displacement curve.

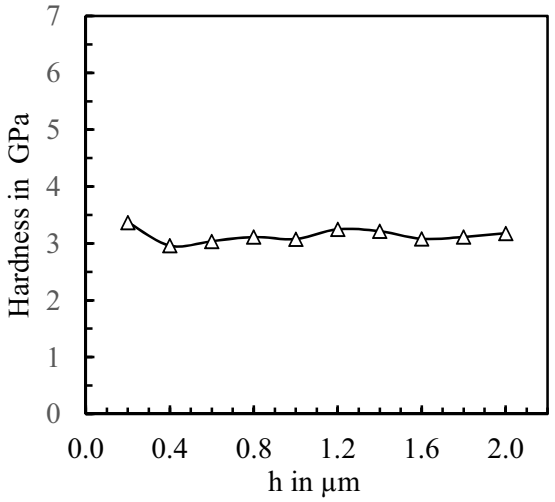

Figure 11. Hardness calculated based on the triangulation method.

5. Conclusions

In this paper three methods are presented to determine the projected area in nanoindentation simulation, namely the Oliver-Pharr method, the A_p-A_c method, and the triangulation method. A Bland-Altman plot shows the agreement of the newly developed triangulation method and the Oliver-Pharr and the A_p-A_c method. However, the Oliver-Pharr method in the presented form is not suited for materials where pile-up is expected to occur. The A_p-A_c method has the disadvantage of neglecting the actual radius of the indenter. It can be concluded that the triangulation method is validated and is the best choice as it takes into account the geometry of the indenter and can handle the appearance of pile-ups. Moreover, it is expected to be suitable for other indenter tip shapes as well. Therefore, it is a versatile method for determining the projected contact area in nanoindentation simulation.

Acknowledgement

The authors would like to thank the Karlsruhe University of Applied Sciences and the Karlsruhe Institute of Technology (KIT) for providing the necessary software and equipment. This research was financially supported by the fellowship of the “Kooperatives Promotionskolleg: Gefügestrukturanalyse und Prozessbewertung” funded by the Postgraduate Research Grants Program of Baden-Württemberg (Germany).

Appendix

A Bland-Altman plot [16] is a suited method to assess the agreement between the three methods. In the Bland-Altman plot, the average of the differences of A_p between two compared methods are plotted against the difference between the particular values of A_p in percent. Furthermore, the mean (correlates to the bias) and the standard deviation (SD) of the difference between two methods are determined. The mean of the differences in the comparison of the triangulation method and the Oliver-Pharr method is at about -5.4%. So, the values for A_p in the triangulation method are on average 5,4% larger than in the Oliver-Pharr method. The mean of the differences in the comparison between the

triangulation method and the A_p-A_c method is at 7.6%, so A_p is on average 7.6% larger in the A_p-A_c method than it is in the triangulation method. The standard deviation of the differences in the comparison of the triangulation and the Oliver-Pharr method is about 3.9%, so about 95% of the determined values for A_p are likely to be in the range of the bias ± 7.8%. In the comparison of the triangulation and the A_p-A_c method, 95% of the values are likely to be in the range of the bias ± 9.6% as the standard deviation is about 4.8%. Beside the comparison of the new method and the established methods, a Bland-Altman plot for the two established methods is prepared. Here, the bias is 12,9% and the standard deviation is 5.1%. The fact, that the bias and the standard deviation in the comparison of the established methods is even larger than in the comparison of the triangulation method with the established methods indicates that the determination of the projected area is a challenging exercise. However, it also proves that the triangulation method is suited for the determination of the projected contact area. The Bland-Altman plots are shown in figure A1.

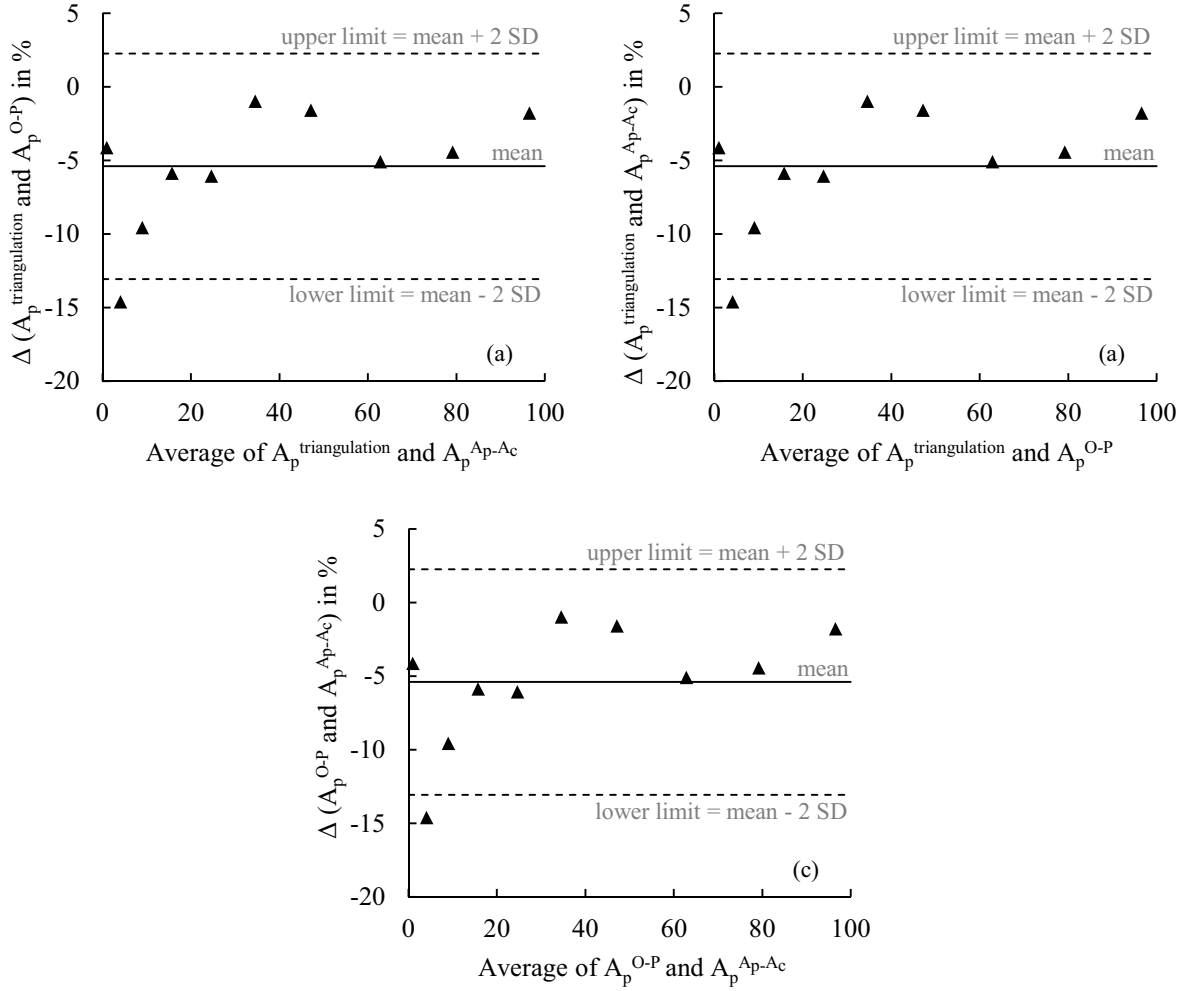

Figure A1. Plot of the difference between the triangulation method and Oliver-Pharr method (a), the triangulation method and the A_c-A_p method (b) and between the Oliver-Pharr method and A_c-A_p method (c) vs. the average of the determined values.

References

[1] Linsmeier C et al. 2017 Development of advanced high heat flux and plasma-facing material *Nuclear Fusion* **57**
[2] Bohnert C, Schmitt N J, Weygand S M, Kraft O and Schwaiger R 2016 Fracture toughness characterization of single-crystalline tungsten using notched micro-cantilever specimens *International Journal of Plasticity* **81** 1-17
[3] Pharr G M, Oliver W C and Brotzen F R 1992 On the generality of the relationship among contact stiffness, contact area, and elastic modulus during indentation *J. Mater.Res.* **7** 613-17
[4] Fischer-Cripps A C 2011 *Nanoindetation* vol 3 (New York: Springer)
[5] Oliver W C and Pharr G M 1992 An improved technique for determining hardness and elastic modulus using load and displacement sensing indentation experiments *J. Mater. Res.* **7** 1564-83
[6] Pethica J B and Oliver W C 1988 Mechanical Properties of Nanometre Volumes of Material: Use of the Elastic Response of Small Area Indentations *MRS Proceedings* **130** 13-23
[7] Oliver W C and Pharr G M 2003 Measurement of hardness and elastic modulus by instrumented indentation: advances in understanding and refinements to methodology *J. Mater.Res.* **19** 3-20
[8] Zhao Z X, Jiang Z D, Li X X and Gao Z K 2006 Calculation of indent's real contact projectionarea in nanoindentation *J. Phys.: Conf. Ser.* **48** 1121-26
[9] Guillonneau G, Kermouche G, Bergheau J-M and Loubet J-L 2015 A new method to determine the true projected contact area using nanoindentation testing *C.R. Mecanique* **343** 410-18
[10] Guillonneau G, Kermouche G, Bec S and Loubet J-L 2012 Determination of mechanical properties by nanoindentation independently of indentation depth measurement *J. Mater. Res.* **27** 2551-58
[11] Liu Y, Wang B, Yoshino M, Roy S, Lu H and Komanduri R 2005 Combined numerical and nanoindentation for determining mechanical properties of single crystal copper at mesoscale *J. Mech. Phys. Solids* **53** 2718-41
[12] Argon A S and Maloof S R 1966 Plastic deformation of tungsten single crystals at low temperatures *Acta Metallurgica* **14** 1449-62
[13] McElhaney K W, Vlassak J J and Nix W D 1997 Determination of indenter tip geometry and indentation contact area for depth-sensing indentation experiments *J. Mater. Res.* **13** 1300-06
[14] Lee W B and Chen Y P 2010 Simulation of micro-indentation hardness of FCC single crystals by mechanism-based strain gradient crystal plasticity *International Journal of Plasticity* **26** 1527-40
[15] Nix W D and Gao H 1997 Indentation size effects in crystalline materials: a law for strain gradient plasticity *J. Mech. Phys. Solids* **46** 411-25
[16] Bland J M and Altman D G 1986 Statistical methods for assessing agreement between two methods of clinical measurement *The Lancet* **327** 307-10